Analysis of the behaviour of a neural network model in the identification and quantification of hyperspectral signatures applied to the determination of water quality.

M.C. Cantero*, R.M. Pérez, P.J. Martínez, P.L. Aguilar, J. Plaza, A. Plaza

Computer Science Dep. Escuela Politécnica. Universidad de Extremadura,
Campus Universitario s/n. 10071 Cáceres. SPAIN.

ABSTRACT

In this work an Unsupervised Neural Computing Model formed by two neural networks is presented: a Self-Organizing Map (SOM) Network and a Hopfield Recurrent Neural Network (HRNN). The first network extracts the endmembers found in the image, analyzing each pixel, and the second network gets the endmember abundances for each pixel in the image. One of the application fields of the proposed methodology is the water quality analysis. In order to study the behaviour of the proposed model, simulation methods have been used to generate hyperspectral signatures from the water spectra obtained in the laboratory. Such data are used for the training and testing of the network. The first sub-network extracts, from the datasets, the endmembers that are used as training patterns in the second one, that provides the matching abundances. The results obtained here will be applied to the treatment of the hyperspectral image Cáceres ES-4, got by the sensors DAIS and ROSIS, from Guadiloba reservoir.

Keywords: water pollution, neural networks, Self-Organizing Map, Hopfield Recurrent Neural Network, hyperspectral data.

1. INTRODUCTION

The present work is clearly a multi-disciplinary study and it intends to join such apparently different subjects as Spectroscopy, Remote Sensing and Neural Networks, applied to water analysis. In this introduction we will try to justify the conexion existing between them, and we will also analyze the antecedents and describe the proposed objectives.

1.1 Water analysis

Water pollution is one of the main ecological problems in our world. The water cycle has so evident a power to clean and purify, and water itself is so abundant, that it has been widely used by men to throw waste products. Rivers and seas have collected from time immemorial the garbage produced by human activity.

Nowadays, the Earth contamination is a global problem in which all the countries must work to gather the best solutions. Thus, technology must be in service of the environment preservation.

If we direct our investigations to polluted water, we must determine the nature and composition of its pollutants, so that we can decide which kind of study will be held. Water pollution has four main origins, three of them are normal and the forth is accidental:

- Animal or human waste, coming from dunghills, stables, etc. The water that has been used with animals does often influence the quality of wells, the nearby springs or superficial terrain layers. Domestic waste water pollutes the rivers, with direct waste or partially depurated waste of treatment installations. This waste provides a contamination formed by materials in suspension, detergents, organic material, bacteria and, in some cases, viruses.
- Water waste or industrial liquid waste, is so very diverse that it includes all known contaminants, radioactive or not, possible carcinogenic agents, mineral or organic, in a proportion that depends on the previous treatment.

* mccantero@unex.es; phone 34 927 257183; fax 34 927 257203

Chemical and Biological Standoff Detection II, edited by James O. Jensen, Jean-Marc Thériault, Proceedings of SPIE Vol. 5584 (SPIE, Bellingham, WA, 2004)
0277-786X/04/$15 · doi: 10.1117/12.580058

- Rain or irrigated waters, that sweep farming contaminants, fertilizers, pesticides, detergents, etc.
- Accidental pollution produced by a concentrated waste of contaminant material, capable of affecting superficial water or water of deep terrain layers.

The numerous contaminants and micro-contaminants that can be found in the water are classified in three categories: mineral contaminants, organic contaminants and viral particles.[1].
The region of Extremadura, placed in the western part of Spain, is mainly an agricultural zone, so the most important contaminants of water are soil fertilizers. The main pollutants present in fertilizers for general purpose are nitrates. These salts are highly nutritious for plants, so they help some water bacteria to develop quickly, and to damage our ecosystems. The movement of nitrate-based compounds from the soil to the aquatic systems affects their balance, and it leads to the decrease of oxygen level of the water, and to the subsequent death of fishes and other aquatic species, and to the loss of bio-diversity. Relating to human beings, drinking water with nitrates causes metahemoglobinemia, a mortal disease for unweaned babies, and more recently it has also been associated with no-Hodgkin lymphoma[1,6].

1.2 Hyperspectral analysis

From a wide point of view, the use of hyperspectral imaging sensor data to study the Earth's surface and its materials is based on the capability of such sensors to provide high resolution spectra, on a per pixels basis, along with the image data. A hyperspectral sensor provides a large number of narrow bands that enable us to recognize such bands of absorption, like in laboratory measurements. This capability can be used to classify and determine the constituent signatures of a material from the hyperspectral information provided by the sensor[2,3].
Hyperspectral images allow us to simultaneously explore the spectral and spatial regularities of the scene[5], but they require enormous storing and transmitting capabilities. A hyperspectral image is equivalent to hundreds of grey-scale images, and each one of its pixels requires various bytes.
The classification and hyperspectral decomposition problems imply, therefore, the realization of search processes in highly dimensional spaces with a high level of noise[4,5].
The decomposition of hyperspectral signatures got by remote sensors (hyperspectral unmixing) as it has been proposed, appeared in the 80's. In the literature we find other names to introduce this subject depending on the field to which it is applied (mixing problem, blind signal separation, sources separation, etc…).
The conventional algorithms have enormous difficulties to manage these data, and it is necessary to use techniques to reduce the dimensionality, such as Principal Components Analysis (PCA) or particular methods of solution based in the generation of synthetic bands with a higher SNR as Minimum Noise Fraction or MNF[5].
In our particular field of application, hyperspectral measurements and experiments offer a wide range of information about water and its quality, specially due to the mentioned variety of their pollutants and, consequently, to their different spectral measurements. Images and training sets can be acquired to examine water composition in different areas, and in consequence their results can help to prevent and to control ecological disasters. In addition, this is a non-destructive technique, and it also prevents the need to make any journey, which reduces its costs compared with other methods of analysis. Due to the range of measurements made in hyperspectral analysis, the wavelengths needed for this study are satisfactorily covered by the method, and not only in a single set of data, but also in a global and periodical way through time and space.
Any object, after receiving some kind of illumination, reflects the light after introducing modifications in it. These modifications are caused by its own structure and composition. The modifications in emitted light radiation generate what is called a hyperspectral pattern. The hyperspectral pattern or signature allow us to interpret the state of the object.
As a method for hyperspectral analysis, linear spectral unmixing (LSU)[8] is one of the most successful approaches to deal with mixed pixels in hyperspectral imagery. The LSU approach involves two steps: the first one is to find spectrally-unique signatures of pure ground components, usually referred to as endmembers in the literature, and the second stage is to express individual pixels as linear combinations of endmembers. One of the new perspectives opened by the LSU approach, together with the improved spectral resolution of sensors, is the possibility of sub-pixel analysis of scenes, which aims to quantify the abundance of different materials in a single pixel.
Due to their complexity, the study of hyperspectral data is very suitable to be treated with neural networks. Neural networks have been widely used with hyperspectral data set and images, because they are a robust and efficient method for their proper analysis.

1.3 Neural networks

Neural network algorithms are frequently used to solve signal separation and classification problems, they are intensive from a computational point of view and they involve a great quantity of iterative calculations, they often get optimum

solutions hard to be obtained with conventional methods[6]. The basic operations that neural networks do are matrix-based like inner and outer product, and this is why they are specially indicated to work with high-dimension vectors as they ones found in hyperspectral images.
During the last decade, artificial neural networks (ANNs) have been successfully applied to the analysis and interpretation of hyperspectral imagery[7,9,10,11]. The advent of ANN approaches in hyperspectral analysis is mainly due to their power in pattern recognition and classification. The pioneering work described by Benediktsson, Sveinson and Arnason[11] demonstrated the effectiveness of Back-Propagation (BP) ANNs for classification of simulated 201-band spectra. Also, Self-Organizing Maps (SOMs)[12] have been recognized as useful tools for classification of images with high spectral dimension. On other hand, full spectral resolution AVIRIS images were classified into a large number of output classes using a similar approach[13]. The mixed pixel problem was tackled by Pendock[14] using an associative ANN to establish a linear mixture model based on endmembers. Despite these attempts, automated determination of endmembers using ANNs has not yet been extensively explored in the literature.
The focus of this paper is to present a LSU approach for the interpretation of hyperspectral imagery based on an unsupervised Neural Computing Model formed by two neural networks: a Self-Organizing Map (SOM) Network and a Hopfield Recurrent Neural Network (HRNN).
The rest of the paper is organized as follows: Sec. 2 illustrates the proposed methodology, Sec. 3 presents the used data, Sec. 4 is for results, and Sec. 5 includes some concluding remarks.

2. METHODOLOGY

In this work is proposed the use of an Auto-Organizative Neural Network (Self-Organizing Map, SOM) for the establishment of hyperspectral reference signatures or "endmembers" of a hyperspectral image, taking advantage of the characteristics that allow this kind of networks to create topological maps from the given input information.
To determine the abundances of each one of the components of the mixed signature, a second Hebbian network is used. This network solves the problem of optimization based in the outputs of the first sub-network. The Hebbian Network (HRNN) works not only with the prototypes but also with the composite signature, and it gets the abundances of each one of the components.

2.1 SOM Neural Network

The network Self-Organizing Maps (SOM's) have been recognized as useful tools for classification of images. This network is based on an unsupervised learning strategy, that finds the similarities between all the studied samples, and it does not require any previous test set. The basic idea of this model is to incorporate, in the competitive learning rule, some sensitivity degree related to the neighbourhood or history. This provides a way of preventing "non-learning" neurons during the training process and, in addition, it favours certain topological properties that must be kept in order to get correspondences between the output neurons and the characteristics of the input patterns[12].
The main objective of the Self-Organizing Map developed by Kohonen is the transformation of a n-dimensional signal or input pattern into a discrete multi-dimensional map, and the adaptive development of this transformation according to some topological ordination criterion.
Each output neuron gets, through the adaptable weight vectors, the information from the input linear neurons layer corresponding to a hyperspectral signature as input pattern x.
The neural model consists of N input neurons and K output neurons, where K is the number of classes or endmembers to be extracted by the network, and must be carefully selected according to image complexity and other metrics[12]. A set of feedforward connections from the input to the output layer, with a set of associated weights (W_{KxN}) are used to perform feature detection. In the output layer, self-feedback and lateral connections produce effects depending on the distance from the winning neuron.
The network processing is given by two different stages: clustering and training. In the clustering step, the feedforward connections project input patterns on the feature space and the Euclidean distance is used to identify a winning neuron. In the training step, lateral and self-feedback connections produce excitatory or inhibitory effects depending on the distance to the winning neuron[10]. It is important to emphasize that the weights associated to feedforward connections will contain the endmember values calculated by the network, after the training phase has finished.
For the training process we use a typical SOM training algorithm[12] with the following characteristics:

- **Weights initialisation**. We choose 0.5 value for the initial weight vectors $\boldsymbol{r_i\ (0)}$, (i = 1,2,...,K).
- **Input pattern selection**: We randomly choose a pixel $\boldsymbol{x}$ belonging to the image.

- **Winning neuron determination**. To find the best-matching (winning) neuron i* at time t, we use a minimum-distance criterion:

$$i^*[x] = \min_{1 \le j \le K} \|x - r_j\|^2 \tag{1}$$

- **Weight adjustment**. Then, the winning and the other neighbourhood neurons adapt their weights closer to the input vector at each learning step using the expression (2), where α(t) and σ(t) are respectively the learning and neighbouring decreasing at the time functions. The winning neuron's weights are modified proportionally to the learning rate. The weights of neurons in its neighbourhood are modified proportionally to half the learning rate

$$r_i(t+1) = r_i(t) + \alpha(t)\sigma(t)\left(x^n - r_i(t)\right) \qquad \text{to} \quad i \in Neighbouring_{i^*} \tag{2}$$

- **Stop criteria:** The SOM training algorithm stops when a pre-determined number of iterations (t) is achieved.

In order to describe the α(t) and σ(t) is necessary to take in account that the learning rate and the neighbourhood are altered during training through two phases:

- **Ordering Phase**. This phase lasts for a certain number of steps. The neighbourhood distance starts as the map size, and decreases slowly. The learning rate starts at the ordering phase learning rate and decreases until it reaches the tuning-phase learning rate. As the neighbourhood distance and learning rate decrease over this phase, the neurons of the network typically order themselves in the input space with the same topology in which they are ordered physically.
- **Tuning Phase**. This phase lasts for the rest of the training steps. The neighbourhood distance reaches the value 1. The learning rate continues to decrease from the tuning phase learning rate, but very slowly. The small neighbourhood and slowly decreasing learning rate fine tune the network, while keeping the ordering learned in the previous phase stable.

In this work, the network will be trained with patterns corresponding to the hyperspectral signatures got in the laboratory, or with patterns of the hyperspectral image Cáceres ES-4, got by the sensors DAIS and ROSIS, and in each case it will create the prototypes corresponding to the endmembers got by the SOM network, and they will be used to form the weight matrix of HRNN, that will be dedicated to get the corresponding abundances.

2.2 Hopfield Recurrent Neural Network

The general solution method to get the endmembers abundances, proposed here, is based on the Hopfield Recurrent Neural Network (HRNN). It is a flexible, efficient and robust approach aimed to solve the problem. The Gradient Method for error reduction is applied to ensure the convergence of the algorithm. The use of this model is fully justified, if we consider that the spectrum formation in the *Pixel Unmixing* is essentially a linear process. The basic difference between the method of steepest descent an the HRNN algorithm is related with the terms of the error.

In order to describe the algorithmic method proposed for Hopfield Recurrent Network, we must previously consider that a mixed hyperspectral signature $\boldsymbol{y}$ can be seen as an N-dimensional vector. This vector is built by sorting the reflectance level associated with each band vs. the band number, where N is the total number of bands:

$$\boldsymbol{y} = [\boldsymbol{y}_1, \boldsymbol{y}_2, \ldots, \boldsymbol{y}_N]^T \qquad y_n \ge 0 \qquad 1 \le n \le N \tag{3}$$

The Endmember Set is referred to as the Reference Matrix R composed by the reference column vectors:

$$R = [r_1, r_2, \ldots, r_K] \tag{4}$$

In a general sense, the set of Composite Pixel is the range of all possible signature that may be produced by a linear combination of all elements belonging to the *Endmember Set*. When the *Endmenber Set* is composed by linearly independent *K* vectors, the result is a *K-dimensional Vector Space*, integrated by all the vectors $\boldsymbol{y}$, and explained as:

$$y = Rc = \sum_{i=1}^{K} c_i r_i \tag{5}$$

where $\boldsymbol{c}$ is the *Abundance Vector*, which is defined as:

$$c = [c_1, c_2, \ldots, c_K]^T \qquad c_k \ge 0 \qquad 1 \le k \le K \tag{6}$$

and where every abundance c_i is a function of the relative intensities of the Composite and Endmember signatures.

Our goal is to estimate $\boldsymbol{c}$, as we assume that $\boldsymbol{R}$ and $\boldsymbol{y}$ are known. For the mixture described by an estimation of $\boldsymbol{c}$, called $\boldsymbol{c'}$, the difference between the measured spectral vector $\boldsymbol{y}$ and its re-constructed version $\boldsymbol{y'}$:

$$\varepsilon = y - y' = y - \sum_{i=1}^{K} c'_i \, r_i \tag{7}$$

is called *Estimation Error,* which gives us a measure of how well the estimation of $\boldsymbol{c}$ has been accomplished. This error is exploited to optimise the estimation process by means of a *Least Mean Square (LMS)* minimization procedure. In relation to $\boldsymbol{c}$, this is laid out to minimise the *Measure Function F(c),* being defined as:

$$F(c) = \|\varepsilon\|^2 = \|y - Rc'\|^2 \tag{8}$$

To solve this problem, we apply an iterative process, supported by the *Linear Hopfield Minimization Procedure*, that is basically a progressive refinement of the *Abundance Vector*:

$$c'(t+1) = c'(t) + \Delta c'(t) = c'(t) + \lambda R^T \left[y - Rc'(t) \right] \tag{9}$$

In compact notation, we can formulate (9) as:

$$\begin{aligned} &\boldsymbol{c(t+1)} = \lambda \boldsymbol{q} + \boldsymbol{P c(t)} \qquad \text{with} \qquad q = R^T y \qquad P = I - \lambda R^T R \\ &\text{where} \quad 1 \le i, j \le K \qquad p_{ij} = -\lambda \sum_{p=1}^{N} r_{pi} r_{pj} \qquad i \ne j \\ &\qquad\qquad p_{ii} = 1 - \lambda \sum_{p=1}^{N} r_{pi} r_{pi} \; q_i = \sum_{p=1}^{N} r_{pi} y_p \end{aligned} \tag{10}$$

in which λ is a parameter dependent on the trace of $\mathbf{R^T R}$. This controls the speed of convergence, whereas $\boldsymbol{p_{ij}}$ denotes the weight from the *i-th* node to the *j-th* node. This method simply requires multiplying and adding operations to solve the *Unmixing Problem*.

In this work, the weight matriz P for HRNN will be built with the endmembers got by the SOM network. To determine the abundances of a certain pixel $\boldsymbol{y}$, the process consists of getting the outputs $\boldsymbol{y}$ calculated by SOM network, that will be the inputs for the HRNN, being its outputs the abundances for each one of the endmembers.

3. RESULTS

Two testing sets have been stablished to evaluate the proposed methodology. In the first place, hyperspectral signatures got in the laboratory have been used to analyze the results of the proposed method, knowing the correct results in advance; and in the second place we have used the data belonging to the image Cáceres ES-4 to try to determine the pollution of the area.

3.1 Laboratory Spectra

The laboratory work in this study included the elaboration of distilled water mixtures with different proportions of a fertilizer containing nitrate, to obtain hyperspectral data belonging to various contamination degrees and, therefore, different variations in pure water spectrum. The spectra of these mixtures was calculated, to know their concentration of nitrate, using Minolta Spectrophotometer CM-508d, and in this way the measurement and illumination conditions were thoroughly controlled. To reduce the measurement errors, 3 different spectral measurements were done for every mixture.

The main contaminant chosen for this experiment was nitrate, due to its massive presence in polluted water in agricultural regions. Nitrates are used as common chemical fertilizers, and Extremadura has a high proportion of cultivated land, to the detriment of industrial areas, so the most interesting pollutants to be taken into account in a study should be fertilizers, pesticides and any kind of product concerning with agricultural uses.

Once the pollutant was chosen, the water mixtures were elaborated following a very simple proceeding. A generic fertilizer with a high nitrate concentration was pounded in a mortar, and the resulting powder was mixed with distilled water, until a saturated dilution (SM) was obtained. It must be taken into account that nitrates are very easily mixed with water, what results in a plain and fast laboratory preparation of the mixtures.

To get the laboratory data, the saturated mixture of nitrate and water was used as polluted water signature. Distilled water (Water) was used as clean water signature. The composition of the mixtures is explained in Tab. 1.

	Water percentage	*SM percentage*
Water	0.97560	0.02439
M1	0.96774	0.03225
M2	0.95833	0.04166
M3	0.91667	0.08334
M4	0.88235	0.11764
M5	0.83344	0.16677
M6	0.75	0.25
M7	0.66777	0.33444
SM	0.50	0.50

Table 1. Water and nitrate composition of the laboratory mixtures.

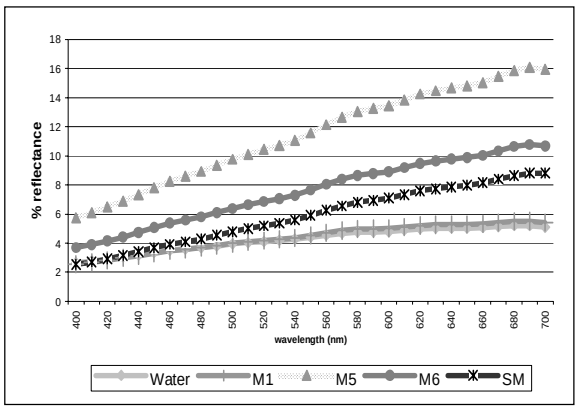

Figure 1. Water and nitrate concentrations in some of the laboratory measurements used for this work.

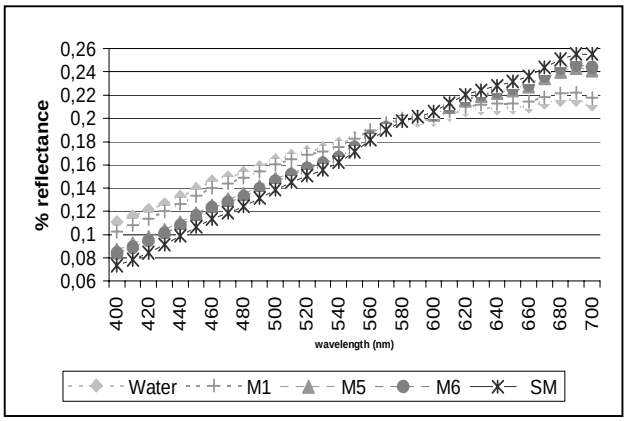

Figure 2. Water and nitrate concentrations, after the normalization, in some of the laboratory measurements used for this work.

The figure Fig. 1 shows the reflectance spectra of the laboratory mixtures used for this experiment. As it can be observed in this figure, it is difficult to appreciate any dependence between the composition of a mixture and its spectra measured in the laboratory. The spectra belonging to similar mixtures are placed in very different positions in the diagram, which hinders its learning using any non-supervised classifier. For this reason, the learning of the spectra shown in Fig. 1 has been attempted using a SOM neural network, with different number of output neurons. The network is unable to distinguish between the endmembers (Water and SM) and the mixture spectra.To avoid the SOM neural network learning the spectra of the mixtures M1 to M7, a pre-processing of the spectra must be done. This process corrects the inappropriate classification problems produced by the use of the Euclidean distance (1).
The figure Fig. 2 shows the normalized spectra of the mixtures used in Fig. 1. It can be seen that the normalized spectra appear in intermediate positions with regard to the endmembers (Water and SM).
To avoid the SOM neural network learning the spectra of the mixtures M1 to M7, a pre-processing of the spectra must be done. This process corrects the inappropriate classification problems produced by the use of the Euclidean distance (1).
The figure Fig. 2 shows the normalized spectra of the mixtures used in Fig. 1. It can be seen that the normalized spectra appear in intermediate positions with regard to the endmembers (Water and SM).

The position of the spectra in Fig. 2 makes it easy to clusterize the sample space and therefore, the pure spectra can be more easily obtained. To get a more accurate information about the relation of the spectra in the training set, the slope of the spectra is represented, for non-normalized spectra in Fig. 3, and for normalized spectra in Fig. 4. The identifiers in these tables of the different measures are (M_i^a M_i^b M_i^c) for a given mixture i. In these figures it is evident that the training spectra can be split into two groups after normalization, what may lead to an easier recognition using SOM neural network. In figure Fig. 4, the first of those groups includes the first 9 patterns in the training set, which have a smaller slope, and the second group starts in the tenth spectra of the set, belonging to the mixture M3 (see Tab. 1).

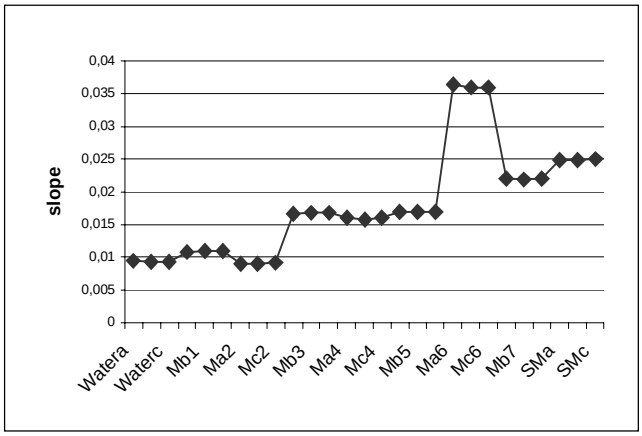

Figure 3.- The slope of the training set spectra before normalization.

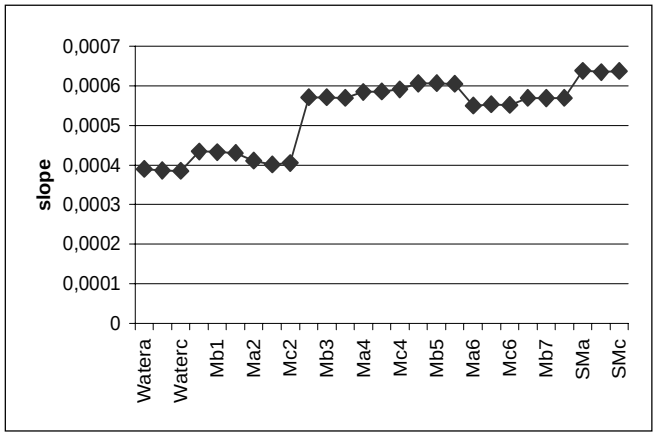

Figure 4.- The slope of the training set spectra after normalization, which help to divide the patterns into two different groups.

Once the pre-processing of the reference set spectra had been finished, the SOM neural network training started. Many trials where carried out, with the aim of determining the behaviour of the neural network when it tries to find the endmembers in the training spectra.

Due to the previously defined characteristics of SOM neural network, after making a great number of tests, it could be concluded that the only network parameter with strong influence in the capacity of finding the endmembers in nitrate dilutions is the number of output neurons.

In the following experiment the results achieved in SOM learning using 2, 3, 4, 5 and 10 neurons are compared. The SOM neural network has been trained using all of the mixtures generated in the laboratory, which belong to the groups Water, M1..M7 and SM (see Tab. 1).

The existence of a relation between the quality of the found endmembers, and their placement in the neurons of the network, is intended to be checked. For this purpose, it can used the Spectral Divergence, between the endmembers and the spectra found in the different neurons.

The Spectral Divergence (SID) is a measure based in the entropies of the spectral signatures[15]. For its correct use, all the vector components must be non-negative (this is valid for radiance and reflectance values). P is the probabilities vector of pixel x. To determine the Spectral Divergence between two vectors, calculating the relative entropy between x and y, the expression (11) must be used.

$$P(x_j) = p_j = x_j \Big/ \sum_{i=1}^{N} x_i \quad \text{Probability vector associated to píxel x}$$

$$P(y_j) = q_j = y_j \Big/ \sum_{i=1}^{N} y_i \quad \text{Probability vector associated to píxel y} \qquad (11)$$

$$D(x \| y) = \sum_{i=1}^{N} p_i \log\left(\frac{p_i}{q_i}\right) \qquad SID(x,y) = D(x \| y) + D(y \| x)$$

To work correctly with these measures, some limitations must be assumed. Firstly, the number of endmembers which suitability is being evaluated must be exactly equal to the number of reference spectra with which the comparison is made, so that the comparison can be made between pairs of hyperspectral signatures. Secondly, the comparison of an endmember must be exclusively made with its corresponding reference signature. Unnecessary comparisons with spectral signatures that provide no information at all must be avoided.

Assuming the hypothesis that the extreme neurons are asymmetric in their neighbourhood, that makes these neurons the ideal candidates for the endmembers storage.

In Fig. 5, only 2 output neurons were used, and it can be seen how the SOM neural network finds endmembers that significantly differ of the experimentally measured endmembers. The endmembers calculated by SOM neural network are placed in an intermediate position, that clearly corresponds to mixture spectra.

In Fig. 6, 3 output neurons were used, and it can be seen that neuron 3 and neuron 1 are closer to the endmembers, as it happens in Fig. 7 with neuron 1 and neuron 3. In Fig. 8, five output neurons were used, being neuron 1 and neuron 3 the closer to the endmembers. Using 10 output neurons (see Fig. 9), neuron 5 and neuron 7 were closer to the endmembers of the training set.

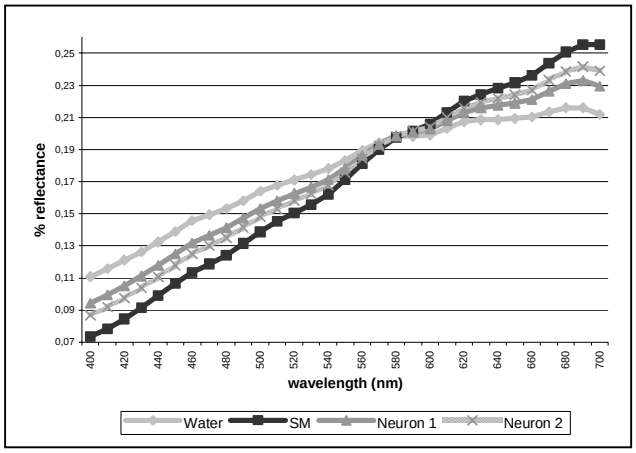

Figure 5. A comparison between the real endmembers of the training set and the results of SOM neural network, when working with 2 output neurons.

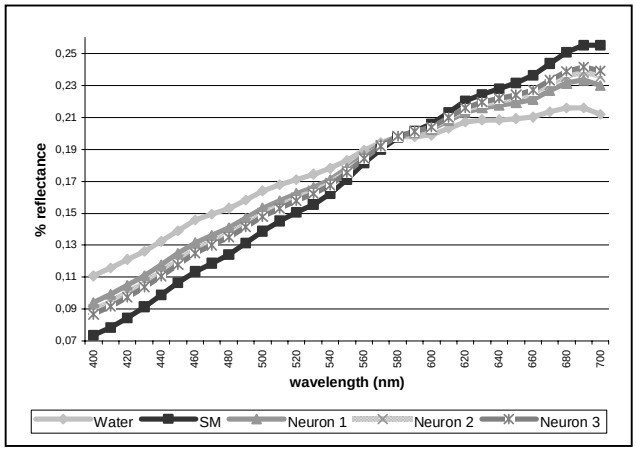

Figure 6. The comparison between SOM neural network results and the endmembers of the training set, with a 3-output neuron network.

From the above discussion it can be deduced that the best endmembers are not always learned in the extreme neurons of the SOM neural network. This can be explained due to the non-uniform distribution of the samples in the spectra vectorial space, despite the normalization process. A solution could consist in doing a pre-selection of the training pattern, to ensure that the generated mixtures are uniformly distributed in the compositions space, and in addition, the distribution should be uniform in relation with the differences between adjacent vectors.

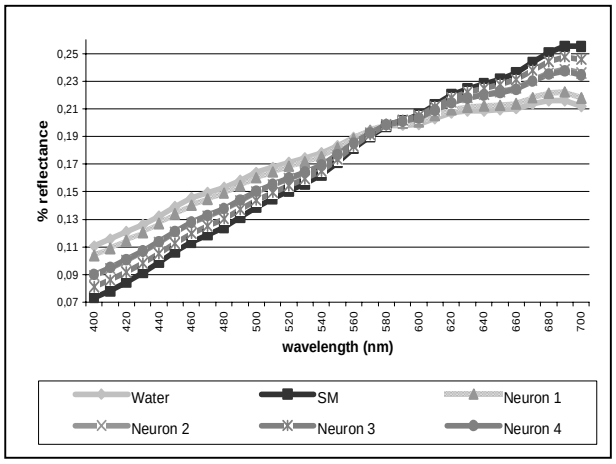

Figure 7. When using a SOM neural network with 4 output neurons, this was the result after comparing the weights of the network with the endmembers spectra.

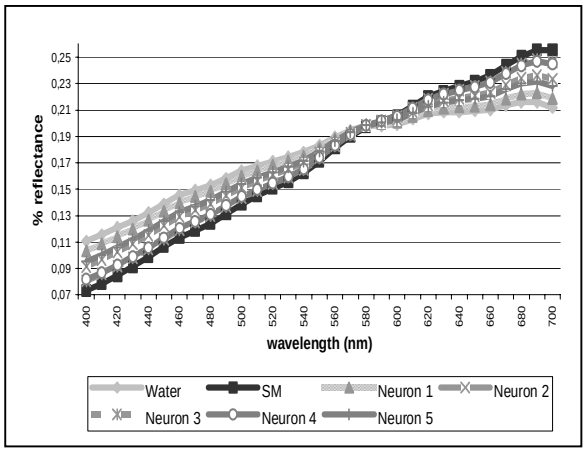

Figure 8. The comparison between the endmembers spectra and SOM weights when using 5 output neurons.

The two endmembers selected by the SOM neural network (E1 and E2) have been used to form the reference matrix ***R***, given in expression (4). The weights and the thresholds that determine the performance of HRNN where calculated using this reference matrix.

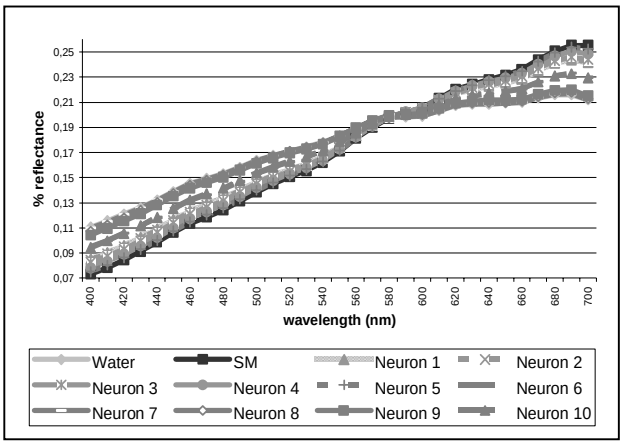

Figure 9. A comparison between the endmembers of the training set and the weights of SOM neural network with 10 output neurons.

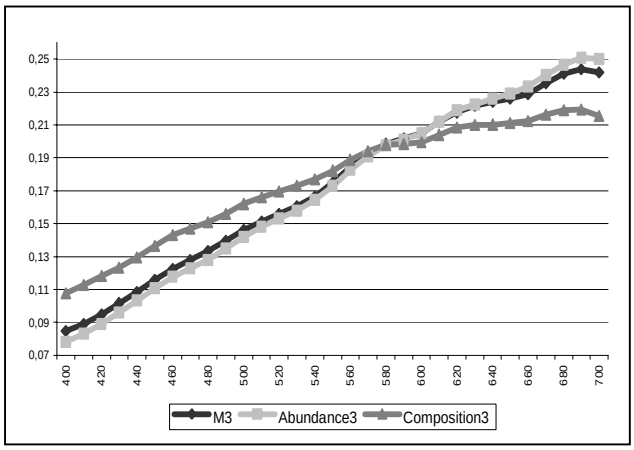

Figure 10. The spectrum of the mixture M3, together with its reconstruction following the laboratory proportions (composition), and its reconstruction using HRNN abundances (abundance).

Due to the fact that the criteria specified in the above paragraph have not been followed in the pattern generation, the only way to ensure a uniform distribution in the weight space, implies the use of a SOM neural network with two output neurons. This, in addition, reduces the calculation time of the network.

In accordance with the algorithm described in Sec. 2.2, M_i ($1 \leq i \geq 7$) mixture spectra where used to determine by the neural network the endmembers abundances, $Ab_i(E1)$ and $Ab_i(E2)$.

To evaluate the quality of the results, a spectrum has been reconstructed with its abundances (see Fig. 10).

The abundance spectrum was reconstructed with the HRNN abundances, following expression (12).

$$\vec{A}_i = \vec{W}ater.Ab_i(\vec{E}_1) + \vec{S}M.Ab_i(\vec{E}_2) \tag{12}$$

The composition spectrum $\vec{C}_i$ was reconstructed assuming a linear-mixture model, following expression (13), where $Comp_i$ is the composition of endmember i with the laboratory proportions of the mixture.

$$\vec{C}_i = \vec{W}ater.Comp_i(\vec{W}ater) + \vec{S}M.Comp_i(\vec{S}M) \tag{13}$$

In Fig. 10 these spectra are compared, and it can be appreciated a greater similarity between Abundance ($\vec{A}_3$) and M3 spectra, being the Composition spectrum ($\vec{C}_3$) slightly different from the others.

Numerically, the spectrum reconstructions can be compared calculating the corresponding spectral divergence, SID(X,A). The table Tab. 2 shows the divergences calculated for the spectra in Fig.10.

	Spectral Divergence
SID(M3, $Abundance_{M3}$)	4.98517e-006
SID($Composition_{M3}$,M3)	0,004427194

Table 2. SID calculations for spectra in Fig. 10.

The mixture represented in Fig. 10 belongs to the most unfavourable case that has been observed. The difference between M3 and $\vec{C}_3$ may be due to non-linear intimate mixture effects.

Once that has been demonstrated the coherence between the results achieved by the network, the proposed model is going to be evaluated. Some of the experiments that were carried out to detect the presence of nitrate in polluted water demonstrate that the exact quantity of this material cannot be calculated. So, the abundances calculated with this model are not quantitative abundances, but they are an approximation of the qualitative presence of nitrate in the mixtures.

3.2 Hyperspectral Image Cáceres-ES4

In this section, the previously described models will be applied to a real image. The image Cáceres-ES4 is dated 28th June 2001, and it was taken with the sensor ROSIS 7915 (VIS-SWIR: 430-860 nm, 115 bands, with a pixel size of

5.6x5.6 m^2). Part of this image shows a very clear and neat view of Guadiloba reservoir, which is an interesting place to test water pollution with nitrate.
In Fig. 11 it can be seen part of the original scene portraying Guadiloba reservoir. One of the grayscale bands of the image (belonging to a wavelength of 544.3 nm) has been chosen to get an accurate view of the zone. The image includes the dam and some possibly polluted zones (indicated in the image), as well as the reservoir itself at different levels of depth. The hyperspectral signatures of the reservoir area have been used to train a SOM neural network with 2 output neurons corresponding to water (from a total number of 4 output neurons), and 80 input neurons, corresponding to the 80 first channels of the ROSIS image, that cover the necessary wavelength to establish a comparison with the results of Sec. 3.1.
In figure Fig. 12, clean water has been identified with the spectra which reflectance levels are slower, in accordance with the results achieved in the laboratory (see Fig. 1). The other spectrum found by SOM neural network can be identified as polluted water, following the same reasoning. In the laboratory experiment, the presence of nitrate was detected thanks to the existence of coloured particles in the nitrate mixture used for the test. These particles presented a shade of brown, and so the spectrophotometer measurements detect a higher radiance in green and, above all, in red wavelengths (from 550 to 700 nm). In the case of Guadiloba reservoir the traces of nitrate have to be found in water alterations. If this is compared with Fig. 1, where the endmembers for water and nitrate are portrayed, we can see that, in the case of Guadiloba reservoir, the difference between the two neurons of water is much slighter. It must be taken into consideration that the water used for laboratory experiments has been previously distilled, so a higher difference between polluted and clean water is expectable.
The massive growth of algae associated with nitrate pollution[16] would very likely increase the levels of green in the water. On the other hand, the growth of algae affects the ecosystem and reduces the oxygen in water, so we can expect the quantity of waste that floats in the water would increase, too. As it can be appreciated in Fig. 12, the spectrum that has been associated with polluted water has higher values of reflectance for wavelengths corresponding to green and red. In Fig. 12 it ca be also observed that the two spectra have, at the beginning, a difference in their angle that is similar to the difference existing in the angle of the endmembers, in Fig. 1.

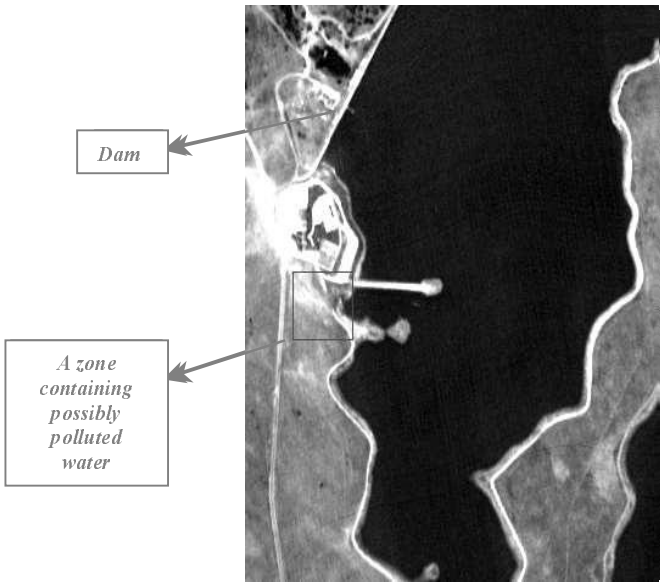

Fig. 11. Guadiloba reservoir portrayed by ROSIS

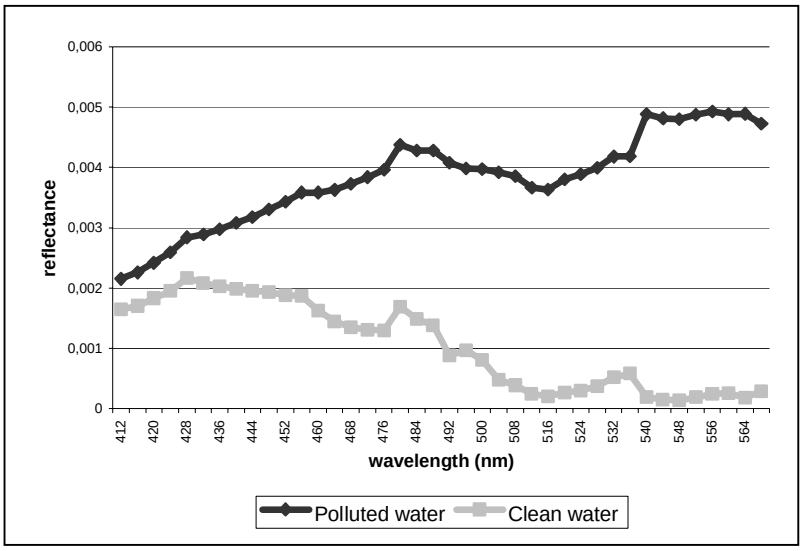

Figure 12. A detail of the first part of the spectra of Guadiloba reservoir water.

The massive growth of algae associated with nitrate pollution[16] would very likely increase the levels of green in the water. On the other hand, the growth of algae affects the ecosystem and reduces the oxygen in water, so we can expect the quantity of waste that floats in the water would increase, too. As it can be appreciated in Fig. 12, the spectrum that has been associated with polluted water has higher values of reflectance for wavelengths corresponding to green and red. In Fig. 12 it ca be also observed that the two spectra have, at the beginning, a difference in their angle that is similar to the difference existing in the angle of the endmembers, in Fig. 1.

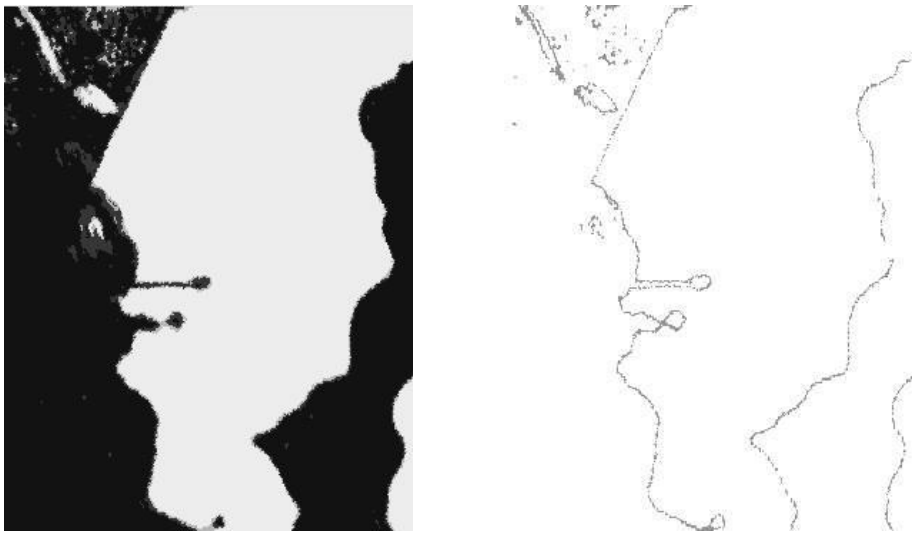

Figure 13. (Left) Guadiloba reservoir after SOM neural network classification, where the land is coloured in black and the water in very pale grey and light grey. (Right) Guadiloba reservoir scene, portraying only the class that could represent polluted water in the SOM neural network classification.

4. SUMMARY AND CONCLUSIONS

In this work polluted water with nitrate has been studied, following two lines of investigation. The first part of the work consisted of a series of measures got in the laboratory, in which polluted water, using a known proportion of nitrate and distilled water, was generated. The resulting spectra were studied and compared in order to distinguish the main

characteristics of the endmembers, using a SOM neural network and a HRNN. The second part of the work dealt with the study of a water reservoir placed in Extremadura, Spain, where the presence of agricultural areas is very high. Thanks to the use of hyperspectral images, some characteristics of water can be detected, and it can be distinguished between water masses suitable of being contaminated with nitrate and clean water zones.
After testing and measuring SOM and HRNN in the detection of polluted water, we can conclude that these methods can be used to identify the hyperspectral signatures of polluted areas in hyperspectral images, and for its localization in a given scene. It must be remarked that this method does not quantify the amount of detected pollutant. First of all, this can be due to the non-linearity of the generated mixtures, and secondly, SOM neural network can also be affected by the non-uniformity of the search space.

5. ACKNOWLEDGEMENTS

This work was supported by the regional government of Extremadura under the PRI 2PR03A061.

6. REFERENCES

1. *Manual técnico del agua*, pp. 605 to 611, Ed. Degrémont, 4th edition, 1979.
2. Goetz, A. F. H., Vane, G., Solomon, J. E., and Rock, B. N., *Imaging spectrometry for Earth remote sensing: Science*, v. 211, 1985 pp. 1147 - 1153.
3. Adams J., Johnson P., Taylor-George S., "A Semi-Empirical Method for Analysis of the Reflectance Spectra of Binary Mineral Mixtures", *Journal of Geophysics Res. 88*, pp. 3557-3561, 1983.
4. Harsany , Chang, "Hyperspectral Image Classification and Dimensionality Reduction", *IEEE Transactions of Geoscience and Remote Sensing*, Vol. 32, pp. 779-785, 1994.
5. Boardman J.W. y Kruse, F.A. "Automated spectral analysis: A geologic example using AVIRIS data, north Grapevine Mountains, Nevada". *Proc. of Tenth Thematic Conference on Geologic Remote Sensing, Environmental Research Institute of Michigan*, Ann Arbor, Vol. I, pp. 407-418, 1994.
6. Haykin S., *Neural Networks: A comprehensible foundation*, Chapter 9, McMillan College Publishing Company, Inc., 1994.
7. Merényi, E., "The Challenges in Spectral Images: An Introduction and Review of ANN Approaches". *Proc. European Symposium on Artificial Neural Networks (ESANN'99)*, pp. 93-98, Bruges, 1999.
8. Petrou, M., Foschi, P.G., "Confidence in linear spectral unmixing of single pixels," *IEEE Trans. Geosci. Remote Sensing*, vol. 37 issue 1 part: 2 , pp. 624 –626, Jan. 1999.
9. Merényi, E., Farrand, W.H., Stevens, L.E., Melis, T.S., and Chhibber, K., "Studying the Potential For Monitoring Colorado River Ecosystem Resources Below Glen Canyon DamUsing Low-Altitude AVIRIS Data," *Summaries of the Tenth Annual JPL Airborne Earth Science Workshop*, Pasadena, CA, February 23-25, 2000.
10. Merényi, E., "The Challenges in Spectral Image Analysis: an Introduction,and Review of ANN Approaches," *Proc. European Symposium on Artificial Neural Networks*, Bruges, Belgium, 1999.
11. Benediktsson, J.A., Sveinson, J.R., Arnason, K., "Classification and Feature Extraction of AVIRIS Data," *IEEE Trans. Geosci. Remote Sensing*, vol. 33, pp. 1194-1205, Sept. 1995.
12. Kohonen, T., *The Self-Organizing Map*, Neurocomputing, vol. 21, pp. 1-6, 1998.
13. E. Merényi, "Self-Organizing ANNs for Planetary Surface Composition Research", *Proc. 6th European Symposium on Articial Neural Networks, ESANN'98*, Bruges, Belgium, 1998.
14. N. Pendock, "A Simple Associative Neural Network for Producing Spatially Homogeneous Spectral Abundance Interpretations of Hyperspectral Imagery", *Proc. European Symposium on Artificial Neural Networks*, Bruges, Belgium, 21-23 April, 1999.
15. Chang, C.-I "An information theoretic-based approach to spectral variability, similarity and discriminability for hyperspectral image analisys", *IEEE transactions on information theory*, vol. 46, 2000.
16. Picone, L.I.; Andreoli, Y.E.; Costa, J.L.; Aparicio, V.; Crespo, L.; Nannini, J.; Tambascio, W., Ria, "Evaluación de nitratos y bacterias coliformes en pozos de la cuenca alta del Arroyo Pantanoso (BS. AS.)", *INTA*, pp. 99-110 ISSN 0325 – 8718, Argentina, April 2003.